Cerebral Cortex September 2015;25:2517–2528
doi:10.1093/cercor/bhu052
Advance Access publication April 23, 2014

Persistence of Functional Sensory Maps in the Absence of Cortical Layers in the Somsatosensory Cortex of *Reeler* Mice

Julien Guy*, Robin J. Wagener, Martin Möck and Jochen F. Staiger

Institut für Neuroanatomie, Universitätsmedizin Göttingen, Georg-August-Universität, Göttingen D-37075, Germany

*Address correspondence to Julien Guy, Center for Anatomy, University Medical Center, Georg-August-University, Kreuzbergring 36, D-37075 Göttingen, Germany. Email: julien.guy@med.uni-goettingen.de

In rodents, layer IV of the primary somatosensory cortex contains the barrel field, where individual, large facial whiskers are represented as a dense cluster of cells. In the *reeler* mouse, a model of disturbed cortical development characterized by a loss of cortical lamination, the barrel field exists in a distorted manner. Little is known about the consequences of such a highly disturbed lamination on cortical function in this model. We used in vivo intrinsic signal optical imaging together with piezo-controlled whisker stimulation to explore sensory map organization and stimulus representation in the barrel field. We found that the loss of cortical layers in *reeler* mice had surprisingly little incidence on these properties. The overall topological order of whisker representations is highly preserved and the functional activation of individual whisker representations is similar in size and strength to wild-type controls. Because intrinsic imaging measures hemodynamic signals, we furthermore investigated the cortical blood vessel pattern of both genotypes, where we also did not detect major differences. In summary, the loss of the reelin protein results in a widespread disturbance of cortical development which compromises neither the establishment nor the function of an ordered, somatotopic map of the facial whiskers.

Keywords: barrel field, cortical blood vessels, intrinsic signal optical imaging, *reeler*, somatotopy

Introduction

Rodents collect tactile information using a set a facial whiskers present on both sides of their snout. Sweeping these vibrissae against objects and surfaces at frequencies within 5–20 Hz enables rodents to perform tasks such as object localization, shape recognition, and texture discrimination (Brecht et al. 1997; Petersen 2007; Diamond et al. 2008; Diamond and Arabzadeh 2013; Feldmeyer et al. 2013). The posteromedial barrel subfield (PMBSF) in the primary somatosensory area of rodents is home to a somatotopic representation of the facial vibrissae on the contralateral side of the snout. A striking feature of this representation is found in the so-called barrel field in the granular layer (layer IV or LIV), where single vibrissae are represented as a dense, discrete cluster of cells called "barrel". Neurons contained within each barrel respond primarily to stimulation of their corresponding whisker (Woolsey and Van der Loos 1970; Welker 1976; Armstrong-James and Fox 1987; Petersen 2007).

In the *reeler* mouse, a homozygous loss of function of the reelin protein leads to abnormal development of the neocortex and other laminated structures characterized by a disturbance and even a loss of cortical lamination (Falconer 1951; D'Arcangelo et al. 1995; Tissir and Goffinet 2003; Dekimoto et al. 2010; Wagener et al. 2010; Boyle et al. 2011). The somatosensory cortex in particular is highly disorganized and devoid of lamination, while retaining columnar organization. Indeed, the barrel field still develops, albeit in a disturbed fashion, and thalamocortical fibers carrying tactile information from the ventral posteromedial thalamic nucleus (VPM) reach the barrel cortex (Caviness et al. 1976; Harsan et al. 2013). It is unclear however, what consequences the loss of cortical layers has on the organization of a functional sensory map in the primary somatosensory cortex and the ability of thalamocortical input to reliably drive cortical network activity.

Intrinsic signal optical imaging (ISOI) is a functional imaging method which, when used in vivo, can measure evoked hemodynamic signals in the cortex and provide insights into its functional architecture (Grinvald et al. 1986; Frostig et al. 1990; Vanzetta and Grinvald 2008). This method has been used to investigate sensory map organization (Masino et al. 1993; Rubin and Katz 1999; Schuett et al. 2002), plasticity (Polley et al. 2004; Drew and Feldman 2009), neurovascular coupling (Martin et al. 2006), and functional connectivity (White et al. 2011) in vivo but also in vitro (Kohn et al. 2000). In the present study, we used ISOI in vivo to explore the organization and function of the somatosensory cortex, and provide the first evidence of somatotopy in the highly disorganized *reeler* barrel cortex from functional imaging in vivo.

Methods

Animals

All experiments were carried out in accordance with German and EU legislation regarding animal research. Three types of experiments were conducted on separate subsets of animals in the present study.

In a first set of experiments, we mapped the functional representation of 9 whiskers, namely C2 and its 8 immediate neighbors, in 6 B6C3Fe wild-type (WT) and 7 B6C3Fe *reeler* mice. A subset of experiments were performed on transgenic animals henceforth referred to as LIV^{tdTomato} either WT or *reeler* ($n = 2$ animals per group). LIV^{tdTomato} animals express tdTomato in LIV neurons, enabling the visualization of the barrel field without the need of any other specific staining. LIV^{tdTomato} were generated by first crossing heterozygous *reeler* animals (B6C3Fe Reln ±) with Scnn1a-Tg3-Cre mice (full strain name: B6.Cg-Tg(Scnn1a-cre)3Aibs/J; Stock Number: 009613, Jackson Laboratory). The resulting Scnn1a-Tg3-Cre *reelers* were then crossed again with each other and animals homozygous for Scnn1a and heterozygous for *Reln* were chosen for further crossings. ROSA-Tomato-LSL mice (full strain name: B6; 129S6-Gt(ROSA)26Sortm9(CAG-tdTomato) Hze/J; Stock number:007905; Jackson Laboratory) were crossed with heterozygous *reeler* in the same way, the resulting strain was called ROSA-Tomato-LSL *reeler*. Crossing of Scnn1a-Tg3-Cre *reeler* and Tomato-LSL *reeler* resulted in LIV specific expression of tdTomato in LIV fated cells. Thus, the respective mouse line was called LIV^{tdTomato}. Heterozygous *reeler* animals were not used for analysis.

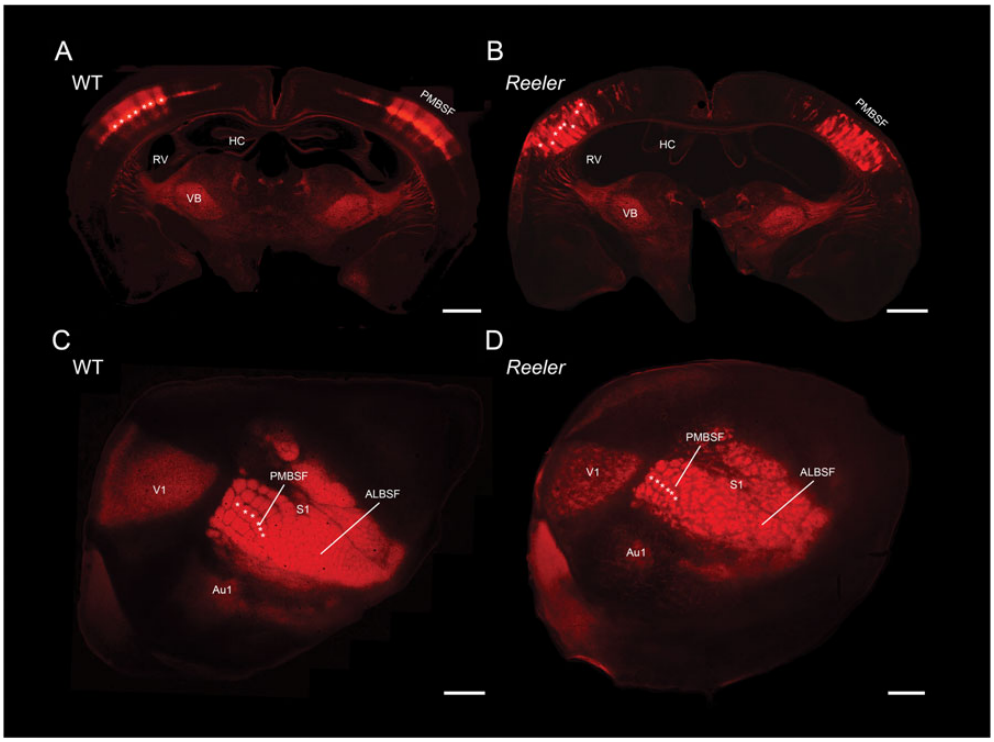

Figure 1. Cytoarchitecture of the barrel field in LIV^{tdTomato} WT and *reeler* mice. (*A* and *B*) Coronal sections through the barrel field of LIV^{tdTomato} WT and *reeler*, respectively. (*C* and *D*) Tangential sections through the barrel field of LIV^{tdTomato} WT and *reeler*, respectively. A subset of barrels and barrel equivalents clusters of dTomato positive cells are marked for comparison (white asterisks). Both sections were obtained from comparable depths of ~400 μm below the pia. ALBSF, anterior lateral barrel subfield; Au1, primary auditory cortex; HC, Hippocampus; PMBSF, posterior medial barrel subfield; RV, right ventricle; V1, primary visual cortex; VB, ventrobasal nucleus. Scale bar: 1000 μm.

In a second set of experiments, we determined the mean amplitude and area of intrinsic signals evoked by stimulating whisker C2 at different, discrete frequencies (see below and Fig. 4). These experiments were conducted on 11 B6C3Fe WT and 12 B6C3Fe *reeler* animals, all adults over 3 months of age and of either gender.

An additional 6 B6C3Fe WT and 6 B6C3Fe *reeler* were used in a further series of experiments where we sought to label the blood vessels in the barrel cortex (see below and Fig. 5).

Surgery

Surgery was performed on all animals used for ISOI experiments ($n = 27$). Mice were anesthetized with intraperitoneal injection of urethane (1.8 g/kg, Sigma-Aldrich, MO) dissolved in a 0.9% sodium chloride solution. Atropine (0.5 mg/kg, Sigma-Aldrich) was injected subcutaneously to minimize breathing impairment caused by urethane. Body temperature was maintained at 37 °C with a heating pad (ATC 1000, World Precision Instruments, Florida) and a life monitoring system was used to monitor breathing rate, heart rate, and blood oxygen levels throughout the experiment (Mouse Ox, Starr Life Science Corp., Pennsylvania). Data obtained during the experiments was discarded if the oxygen saturation level dropped below 80%. Lidocaine (Xylocaine 2%, AstraZeneca, Germany) was injected subcutaneously under the scalp. The scalp was dissected out to reveal the skull, and a custom built head post was attached to the right side of the skull with cyanoacrylate adhesive to facilitate head fixation during imaging. The skull over the left somatosensory cortex was carefully thinned to transparency with a dental drill (OS-40, Osada Electric Company, Japan) under regular cooling from a 0.9% sodium chloride solution. A ring of dental cement was raised around the resulting cranial window, filled with saline, topped with an 8 mm diameter round cover glass (Electron Microscopy Sciences, PA) and sealed with Vaseline, thus forming an optical chamber through which illumination of, and image acquisition from the somatosensory cortex was possible. The whiskers on the contralateral side of the snout were shaved except C2 and its 8 immediately adjacent neighbors, which were trimmed to ~1 cm in length instead.

Whisker Stimulation

Whisker stimulation was achieved by inserting individual whiskers into a glass capillary (1.5 mm outer diameter, World Precision Instruments, Florida) glued to a piezo actuator activated by a computer controlled amplifier (E-650 LVPZT, Physik Instrumente, Germany). Stimulation consisted in rostro-caudal deflections of ~1 mm, delivered for 2 s at controlled frequencies (1, 5, 10, or 25 Hz).

Intrinsic Signal Optical Imaging

In order to acquire images from the cortex, we used a CCD camera (Adimec 1000 m, Adimec, The Netherlands) mounted on a tandem lens assembly composed of a 50 mm Nikon bottom lens adapted on a 135 mm Nikon top lens for a final magnification of ×2.7. The maximum resolution of the CCD camera was 1000 × 1000 pixels with a final pixel size of ~2.8 × 2.8 μm. The CCD camera was coupled to an Imager 3001 data acquisition system (Optical Imaging, Israel). We obtained pictures of the superficial blood vessel pattern by focusing the camera on the pial surface while illuminating the cortex with a 100 W halogen lamp with stable power supply (Kepco ATE 15–15 M, Kepco, Japan), filtered through a 546 nm filter, in order to enhance contrast between blood vessels and surrounding parenchyma. For functional imaging, the focal plane was subsequently moved 300 μm below the pial surface and the illumination wavelength was changed to 630 nm by exchanging filters. The light intensity was adjusted to just below camera saturation in every experiment.

Two data sets were obtained from our experiments. When mapping cortical representation of 9 individual whiskers in LIV^{tdTomato} animals, ($n = 17$), full resolution data frames were acquired at a rate of 50 frames per second (fps) and binned to a rate of 5 fps. Data acquisition started 0.2 s after stimulation onset and lasted 2 s, with 30 s between individual trials, and the stimulation was delivered at 5 Hz for 2 s. 30 trials were averaged in order to improve signal-to-noise ratio. This data set was used to localize the functional representations of individual whisker with respect to one another.

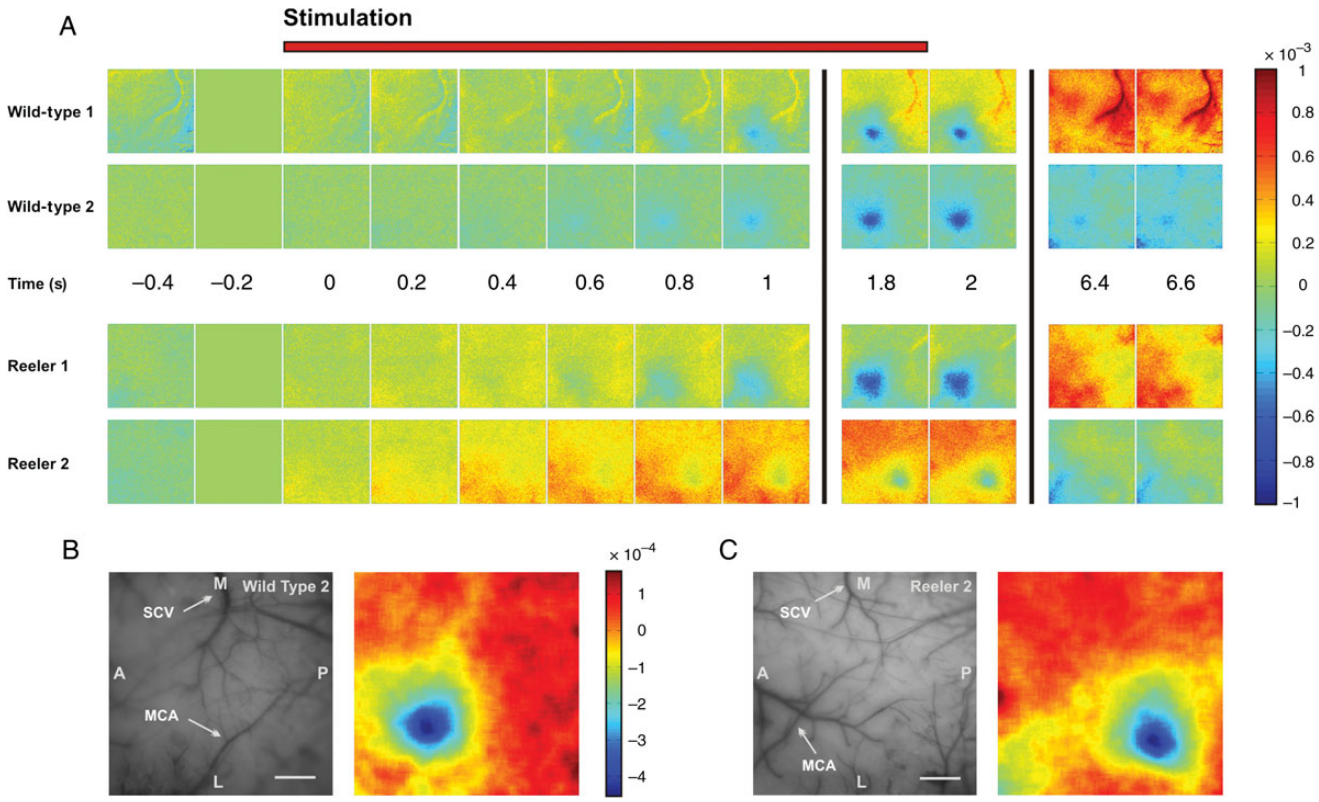

Figure 2. The hemodynamic response to single-whisker stimulation in WT and *reeler* mice. (*A*) Time series of camera frames illustrating the response to stimulation of whisker C2 at 5 Hz for 2 s in 2 representative examples of WT and *reeler* animals. Stimulation starts at time 0, each frame represents 200 ms. The camera frame immediately before stimulation onset was used as reference for normalization; the scale bar represents fractional change in reflectance with respect to that frame. Stimulation evoked a localized hemodynamic response corresponding to the sensory representation of whisker C2 in WT but also in *reeler* mice. Neither the mean latency nor mean duration of the evoked intrinsic signal differed significantly between genotypes (one-way ANOVA, P = 0.7 and P = 0.46, respectively). (*B* and *C*) Left, photograph of the surface vasculature in 2 representative examples corresponding to the data in *A*. SCV, superior cerebral vein, MCA, middle cerebral artery, M, medial, L, lateral, A, anterior, P, posterior. Scale bar: 500 μm. Right, sensory maps obtained by binning 15 frames spanning the period from 1 to 4 s after stimulation, applying Gaussian blur with σ = 86 μm and subtracting the median of the filtered image.

In another set of experiments, a separate data set was obtained on which to quantify the amplitude and area of the intrinsic signal evoked by whisker stimulation ($n = 11$ B6C3Fe WT and 12 B6C3Fe *reeler*). In these experiments, data frames were acquired as described above with an additional 9 × 9 spatial binning. Data acquisition started 15 s before stimulation onset and lasted 36 s, with 60 s between individual trials. Whisker stimulation lasted 2 s and was delivered to whisker C2 at varying frequencies (see below). 20 trials were averaged for every stimulus condition. Whisker stimulation and data acquisition were synchronized with custom written LabVIEW routines (National Instruments, TX).

Perfusion and Tissue Collection

At the end of the imaging experiments, animals were given an overdose of urethane intraperitoneally and were transcardially perfused with 10% sucrose followed by a 4% paraformaldehyde (PFA) solution containing 15% (v/v) picric acid in 0.1 M phosphate buffer (PB). The brain was collected; the cortex over the left hemisphere was dissected out, flattened, and postfixed overnight in the same fixative (Welker and Woolsey 1974).

Animals used for staining of blood vessels were given an overdose of ketamine hydrochloride intraperitoneally and decapitated before the brain was dissected out and fixed by immersion in 4% PFA-15% picric acid in 0.1 M PB overnight.

Histochemistry

4′,6-Diamidino-2-phenylindole (DAPI) staining was carried out on tissue collected from $LIV^{tdTomato}$ animals. The flattened cortex was cut in 100 μm thick tangential sections on a vibratome (VT1200S, Leica, Germany), collected and rinsed in PB buffer (pH 7.4). DAPI staining was done according to the manufacturer's specifications (Molecular Probes, Oregon), before the sections were mounted and coverslipped with Aqua-Polymount (Polysciences, Pennsylvania). Because LIV fated cells constitutively express dTomato in $LIV^{tdTomato}$ animals, no further staining was necessary to reveal the barrel field.

The tissue obtained from animals used in the blood vessel quantification ($n = 6$ animals per group, see Fig. 5) was stained with DAB (diaminobenzidine tetrahydrochloride dihydrate, Roth, Germany). Serial, 100 μm-thick coronal sections containing the barrel field were cut on a vibratome, collected and rinsed several times in PB (pH 7.4). They were subsequently incubated for at least 90 min in 0.01 M phosphate-buffered saline containing 25% saccharose and 10% glycerol, followed by 3 freeze/thaw cycles on dry ice. After rinsing with PB (3 × 15 min), 0.05 M TRIS buffer (TB, pH 7.4, 15 min) and TRIS-buffered saline (TBS, pH 7.4, 2 × 15 min), the sections were incubated overnight at 8 °C in TBS containing avidin and biotinylated horseradish peroxidase diluted at 1:400 each (ABC Vectastain, Vector Laboratories, California). Sections were recovered the next day, rinsed in TBS for 20 min and thrice in TB for 20 min, before incubation with 0.5 mg/mL DAB in TB. The reaction was started by adding 1 μL TB containing 1% hydrogen peroxide, allowed to develop under regular visual control, and stopped by rinsing thrice in TB. We proceeded with a cytochrome oxidase staining as described by Wong-Riley and Welt (1980). Finally, the sections were mounted and coverslipped with Aqua-Polymount.

Data Analysis

Analysis of intrinsic signals was performed with custom written MATLAB programs (The MathWorks, Massachusetts). Series of camera frames were normalized using the following formula: $\Delta R/R_o = (R - R_o)/Ro$, where $\Delta R/R_o$ is the fractional change in reflectance from reference, R is the light reflected during any given frame and R_o the light reflected

during the reference frame immediately preceding whisker stimulation onset.

The data obtained from experiments on LIV^{tdTomato}, where the localization of the functional representations of 9 individual whiskers was recorded, was processed in the following way. The 5 data frames spanning 1.2–2.2 s after stimulation onset, when the intrinsic signal is clearly visible (Fig. 2), were averaged. A Gaussian filter ($\sigma = 86$ μm) was applied to the resulting frame to improve threshold detection, and the median of the data frame was subtracted to minimize the effect of noise, especially the slow spontaneous oscillations in reflectance (Mayhew et al. 1996; Drew and Feldman 2009). In order to localize the intrinsic signals evoked by stimulation of different whiskers with minimal overlap, we extracted the contour lines encompassing the area where the signals were at 90% of their maximum (Fig. 3 and Chen-Bee et al. 2000).

In order to map intrinsic signals on the barrel field, we reconstructed the barrel field and pial vascular network from serial tangential sections of LIV^{tdTomato} mice cortex under the ×5 objective of an Axio Imager M2 microscope (Zeiss, Germany) using the Neurolucida software (MBF Bioscience, Vermont). Before mapping the location of sensory evoked signals on the reconstructed barrel field, we used a warping algorithm written in MATLAB and designed to align the reconstructed pial vascular network to the one photographed during the experiment, using a set of fiducial points in order to partly compensate for the curvature of the brain and distortion of the tissue (see Fig. 3).

The data obtained from B6C3Fe animals and used for quantifying the amplitude and area of the response evoked by stimulation at varying frequencies was treated as described above, with a few notable differences. The 15 frames spanning the 1–4 s after stimulation onset were averaged, and a Gaussian filter with $\sigma = 130$ μm was applied to the resulting frame because of the lower spatial resolution resulting from the spatial binning procedure. The median of the resulting frame was subtracted. We measured the response amplitude as the peak dR/R_o value in the resulting data frame, which was always located within the region activated by whisker stimulation, and fixed thresholds (1, 2, 3, 4, and 5 × 10e−4) where applied to all experiments for area measurements (see Fig. 4 and Chen-Bee et al. 2000).

Images of coronal sections stained with DAB and used for blood vessel density analysis were acquired with the ×5 objective of an AXIO Imager M2 microscope and digitized with an AXIO cam MRm CCD camera (Zeiss). Minimum intensity projections were obtained from stacks of pictures acquired in 5 μm steps through the thickness of each individual 100 μm thick sections ($n = 6$ animals per group). We

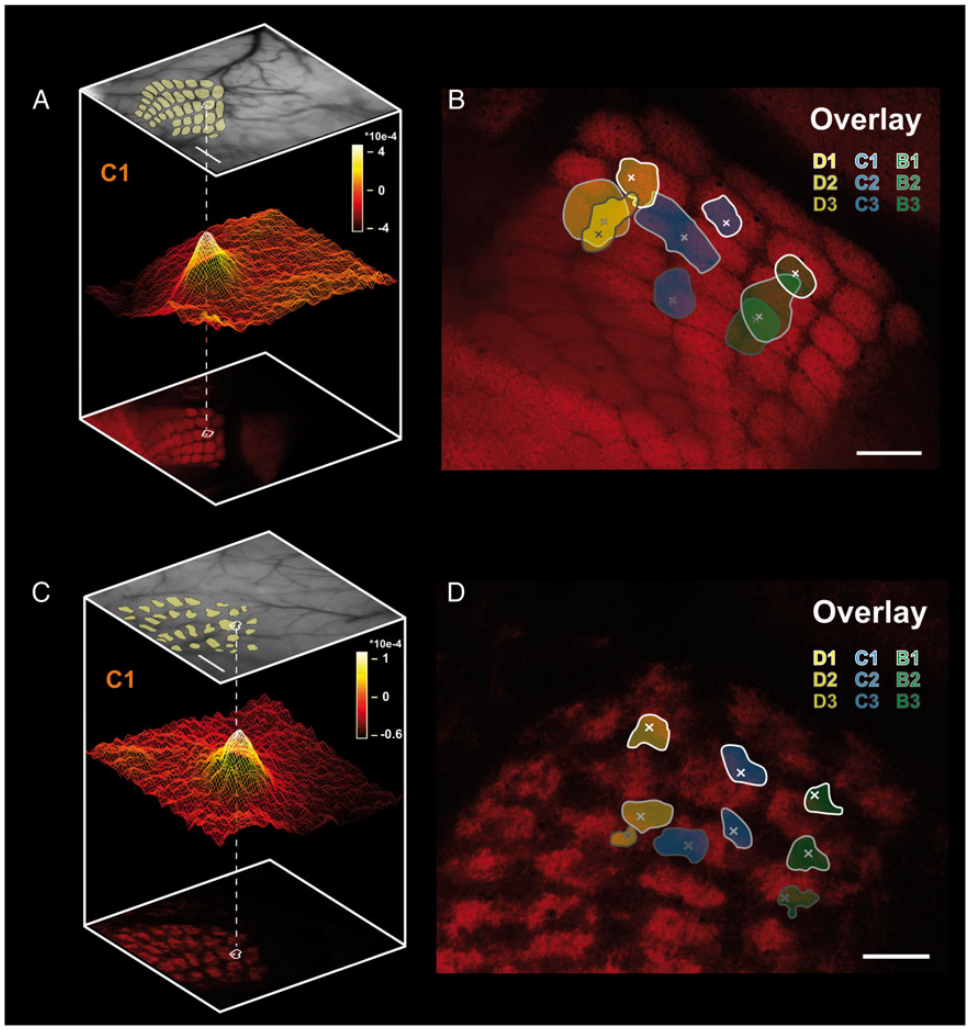

Figure 3. Sensory map organization in WT and *reeler* somatosensory cortex. (*A* and *C*) Pseudo 3D-reconstruction of the location of the hemodynamic response evoked by single-whisker stimulation with respect to the barrel field in WTand *reeler*, respectively. Top: photograph of the superficial blood vessels acquired during the experiment under a 546 nm wavelength illumination (scale bar: 500 μm). Bottom: the barrel field was reconstructed postmortem from tangential sections through the barrel cortex of LIV^{tdTomato} mice. Middle: surface plot of the averaged intrinsic signal evoked by stimulating the C1 whisker at 5 Hz for 2 s (scale bar in absolute values). The location of the peak and 90% of maximum isoline were mapped on the barrel field after aligning the blood vessels present in the reconstructions of the serial tangential sections with those present in the pial surface photograph of the living animal. (*B* and *D*) overlay of peak (x) and 90% maximum isolines locations of 9 intrinsic signals evoked by sequential stimulation of 9 whiskers in the same WT and *reeler* mouse, respectively. The spatial relationship between the functional intrinsic signals locations show a rough match with those of individual structural barrels. Scale bar: 250 μm.

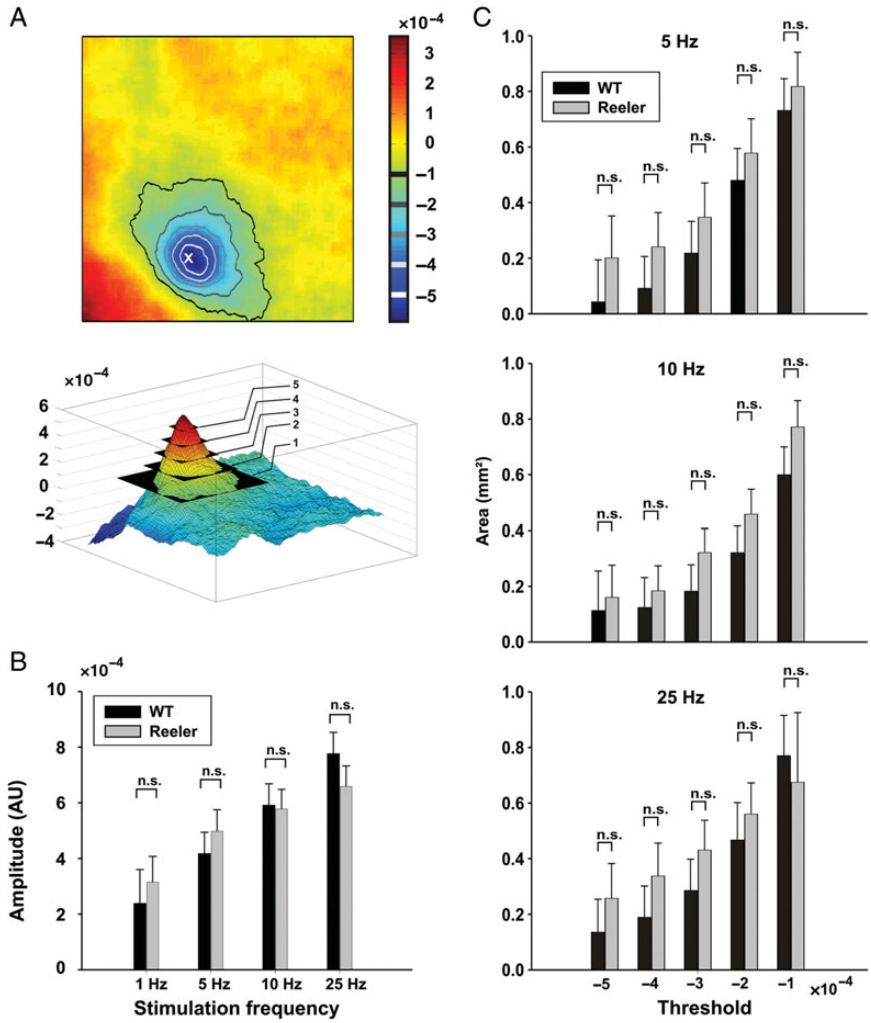

Figure 4. Stimulus representation in WT and *reeler* mice. (*A*) Top, representation of whisker C2 overlaid with threshold isolines. The level of subsequent thresholds is indicated on the scale bar, which represents fractional change in reflectance. The asterisk labels the peak amplitude of the evoked response. Bottom, same data as top in absolute value. (*B*) Peak amplitude of evoked response (in fractional change in reflectance, absolute value) as a function of stimulation frequency (mean ± standard error of mean [SEM], n.s.: nonsignificant, ANOVA, $P = 0.71$). (*C*) Area encompassed within isolines of thresholds indicated in *A* as a function of stimulation frequency (in mm^2, mean ± SEM, n.s.: nonsignificant, ANOVA, $P = 0.12$, $P = 0.09$, and $P = 0.35$ for 5, 10, and 25 Hz, respectively). The 1 Hz stimulation frequency did not evoke responses that consistently reached threshold values and is therefore not represented here. $N = 11$ WT and 12 *reeler*.

examined 6 successive coronal sections through the barrel field in each animal. A threshold detection algorithm written in MATLAB was applied to calculate the relative section surface occupied by stained erythrocytes and thus blood vessels within selected regions of interest (ROIs). Briefly, the surface of the pia over the barrel field was manually outlined in pictures of coronal sections. The algorithm automatically generated successive, 100 µm-thick ROIs starting at the outline of the pia and covering the entire cortical thickness. The number of pixels detected above threshold in each successive bin was divided by the total number of pixels in that bin, resulting in an estimate of blood vessels density in dimensionless numbers reported as arbitrary units (see Fig. 5).

Statistical analysis was carried out with SigmaPlot (Systat Software Inc., Illinois) and STATISTICA (Statsoft, Oklahoma) software with a significance threshold at $P = 0.05$.

Results

Cytoarchitectonic Features of the Barrel Field in Reeler *and WT Mice*

In order to visualize the cytoarchitecture of the barrel field in both genotypes, we took advantage of our $LIV^{tdTomato}$ reeler and WT mice lines, in which Cre recombinase is expressed under the Scnn1a promoter (nonvoltage gated sodium channel, subunit alpha) while dTomato is expressed in a Cre-dependent manner (Madisen et al. 2010). The resulting distribution of dTomato positive cells is illustrated in Figure 1, where Figure 1*A*,*C* are photographs of coronal and tangential sections through the somatosensory cortices of a WT mouse, respectively. In the coronal section, dTomato positive cells are found in LIV of the neocortex and to a lesser degree in thalamic structures, with the strongest expression located in the posterior medial barrel subfield (PMBSF). More specifically, dTomato positive cells form clusters, or barrels, in LIV of the PMBSF (examples are marked with white asterisks in Fig. 1). Such structures are also obvious in a tangential section through the PMBSF (Fig. 1*C*), where the characteristic barrel field, organized in arcs and rows, is visible and individual barrels can indeed be recognized (Woolsey and Van der Loos 1970; Welker 1976). Thus, dTomato expression appears to be enriched in LIV of the $LIV^{tdTomato}$ mouse cortex and can hence provide a mean to reliably identify single barrels in WT

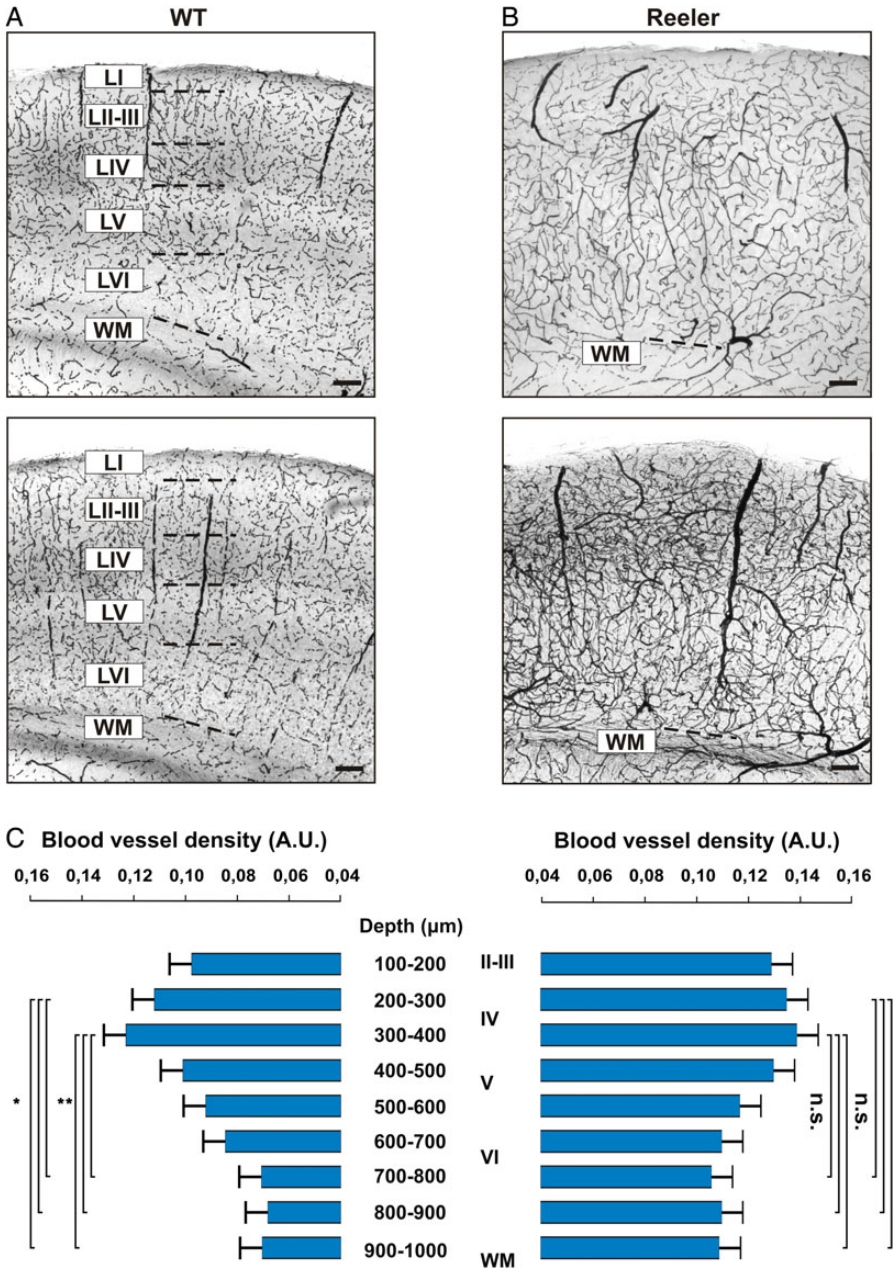

Figure 5. Vascular network in the barrel cortex of WT and *reeler* mice. (*A* and *B*) Coronal sections through the somatosensory cortex of 2 representative WT and *reeler* mice, respectively ($n = 6$ in each group). DAB staining was used to stain erythrocytes in an unperfused brain, providing an indirect but efficient way of revealing the vascular network of the somatosensory cortex. wm: white matter. Scale bar: 100 µm. (*C*) Relative density of blood vessels as a function of depth in WT (left) and *reeler* (right) animals. Density was calculated in 100 µm bins from the pia to the white matter. The first 100 µm below the pia were excluded because a heightened background was consistently found near the pia.

animals and their equivalents in *reeler*. Clusters of dTomato expressing cells are also present in the cortex of *reeler* animals (Fig. 1*B*) although they are not restricted to a single layer but rather span almost the entire cortical thickness, in agreement with the loss of lamination characteristic of this mutant (Dekimoto et al. 2010; Wagener et al. 2010; Boyle et al. 2011). These clusters are also visible in tangential sections (Fig. 1*D*) where they form a recognizable barrel field. A previous study from our laboratory established that barrel equivalents in *reeler* have a significantly less symmetrical shape than their WT counterpart, are smaller, but occupy a proportionally equivalent size when taking the overall hypotrophy of the *reeler* brain into account (Wagener et al. 2010). The cellular composition of the *reeler* cortex has been the subject of scrutiny as well, revealing for instance that the total number of cells within a radial column does not differ from WT (Goffinet 1984; Polleux et al. 1998). Although the composition of the cortical neuronal population has been shown to differ between genotypes, with a relative increase in the proportion of late generated neurons and a corresponding decrease in the share of early generated neurons in *reeler* (Polleux et al. 1998), the number of LIV equivalent cells, which form barrel-like clusters, does not differ from WT (Wagener et al. 2010). Overall, the main cytoarchitectonic feature of the *reeler* barrel field is a disturbance

of its radial organization while its tangential organization is essentially preserved (Caviness et al. 1976; Caviness and Rakic 1978; Wagener et al. 2010; Boyle et al. 2011).

Sensory Map Organization in Reeler *and WT Mice*

Our surgical procedures allowed us to prepare optical chambers over the barrel cortex which enabled acquisition of detailed images from the cortex where individual vessels were clearly recognizable (Fig. 2*B*,*C*, left). Figure 2 A shows representative results of intrinsic signals evoked by stimulation of whisker C2 in 2 WT and 2 *reeler* mice under urethane anesthesia. Variations in blood volume and hemoglobin oxygen saturation levels are expressed as changes in reflectance with respect to a reference frame corresponding to the 200 ms preceding stimulation onset (time: −0.2 in Fig. 2), such that increases in blood supply and oxygenation following enhanced neuronal activity, which locally cause an increase in light absorption, are represented in blue shades. The intrinsic signal recorded across entire camera frames over time comprised several components, such as spontaneous variations in blood supply to the cortex and vascular artifacts (visible in the later frames of WT 1, for instance). In addition to these spontaneous components, we were able to reliably record hemodynamic signals evoked by sensory stimulation and appearing as spatially restricted increases in blood supply and oxygenation (see frames 1.8 and 2). We investigated the temporal dynamics of the intrinsic signal by measuring its latency and duration for comparison between genotypes. The intrinsic signal typically became visible within 1 s of stimulation onset and returned to baseline within ∼10 s of stimulation onset in both groups. Neither response latency nor response duration were significantly different when comparing genotypes (mean onset latency and standard deviation (SD): 0.76 ± 0.15 s in WT, 0.73 ± 0.1 s in *reeler*, one-way analysis of variance (ANOVA): $P = 0.7$; mean duration and SD: 8.9 ± 1.7 s in WT, 8 ± 2 s in *reeler*, one-way ANOVA: $P = 0.46$; $n = 10$ and 9 for WT and *reeler*, respectively). The time course of the intrinsic signals in *reeler* is therefore very similar to that in WT.

We next used ISOI to determine whether somatotopy exists in functional maps in the WT and *reeler* barrel cortex. Indeed, by binning 15 frames spanning 1–4 s from whisker stimulation onset, it was possible to reliably extract spatially restricted intrinsic signals corresponding to the sensory representation of the stimulated whiskers in the imaged cortex (Fig. 2*B*,*C*, right). Therefore, we stimulated an array of 3×3 whiskers (centered on C2 because of its central position in the whisker pad) in $\text{LIV}^{\text{tdTomato}}$ animals, which enabled us to determine whether their functional representations were aligned along rows and arcs in the same manner barrels are aligned in the barrel field. In addition, we reconstructed the barrel field and superficial blood vessel pattern from tangential sections (representative examples are shown in Fig. 3*A*,*C*). By aligning the reconstructed superficial vasculature with that photographed during the experiment, it was possible to map the localization of any given whisker representation on the barrel field. Hence, we could examine the spatial relationships of functional whisker representations with one another in functional maps and compare the resulting pattern with that formed by barrels in the anatomical barrel field.

In WT animals, sequential stimulation of whiskers along a row, for instance whiskers B1 to B3, yielded intrinsic signals which were aligned along a "row axis". This alignment matched that observed between the corresponding barrels in the anatomical barrel field (Fig. 3*B*). In addition, sequential stimulation of whiskers along an arc, such as whiskers D1, C1, and B1, evoked intrinsic signals that were also aligned along an "arc axis" similar to that defined by their corresponding barrels. In both the functional and anatomical maps of the whisker pad, the row and arc axis intersected at a roughly perpendicular angle. These similarities between the functional and anatomical maps constitute evidence for the existence of somatotopy at the level of functional sensory maps, as previous authors have demonstrated (Masino et al. 1993).

How is the sensory map of the whisker pad spatially organized in the otherwise highly disorganized *reeler* barrel cortex? We applied the same sequential stimulation of 9 whiskers to *reeler* animals (Fig. 3*D*) to probe the spatial relationships of their functional representations. Stimulation of whiskers along a row evoked intrinsic signals which were aligned, as they were in WT. Upon stimulating whiskers along an arc, the same alignment of their functional representations was observed than in WT. Similarly, the row and arc axis in *reeler* also intersected at a roughly perpendicular angle. It can be concluded from these observations that the spatial organization of functional sensory maps in *reeler* is essentially the same as in WT. The most parsimonious explanation for this finding is that like its WT counterpart, the *reeler* barrel cortex remains organized as a somatotopic representation of the whisker pad in spite of the otherwise extensive disruption of its laminar organization.

A degree of mismatch exists between the functional and the anatomical maps however, in that the peak of the intrinsic signals rarely perfectly matched the barrel centers. This can be explained by at least two facts. One the one hand, the exact location of the center of an intrinsic signal evoked by single-whisker stimulation is determined not only by the center of the corresponding barrel, but also by the location of the nearest penetrating arteriole (Blinder et al. 2013), suggesting that a small degree of "built in", physiological mismatch when using this method may be detected in the barrel field. On the other hand, the accuracy of our reconstructions and warping algorithm are limited. Any inaccuracies in the alignment of successive serial sections or in the alignment of blood vessels during the warping process are likely to add up and contribute to the observed mismatch. This technical component is likely the primary contributor to the shift observed in our experiments. The mismatch itself, however, bears little consequence on the observation that WT and *reeler* functional maps are highly similar in their spatial domain and the ensuing conclusion that somatotopy exists in the *reeler* barrel cortex, and should not be interpreted as illustrating a biological mismatch between structural and functional maps (Dubroff et al. 2006).

Single-Whisker Stimulus Representation in Barrel Cortex

How is a discrete parameter of individual whisker stimulation such as frequency represented in the *reeler* barrel cortex? We investigated this question by stimulating whisker C2 for 2 s at frequencies of 1, 5, 10, and 25 Hz, a frequency range that overlaps with spontaneous whisking as observed in awake behaving rodents (Carvell and Simons 1990), and measured the peak amplitude of the response (Fig. 4*A*,*B*). The amplitude of the response increased with increasing stimulation frequency in both genotypes. The range of the peak amplitude of the

Table 1
Cortical area covered by intrinsic signal evoked by whisker stimulation at different frequencies in *reeler* and WT

Genotype	WT			*Reeler*		
Frequency (Hz)	5	10	25	5	10	25
Threshold ($\times 10^{-4}$)						
−5	0.04 (0.15)	0.11 (0.14)	0.13 (0.12)	0.20 (0.15)	0.16 (0.11)	0.26 (0.12)
−4	0.09 (0.11)	0.12 (0.11)	0.19 (0.11)	0.24 (0.12)	0.18 (0.09)	0.34 (0.12)
−3	0.22 (0.11)	0.18 (0.09)	0.28 (0.11)	0.35 (0.12)	0.32 (0.08)	0.43 (0.11)
−2	0.48 (0.11)	0.32 (0.09)	0.47 (0.13)	0.58 (0.12)	0.46 (0.09)	0.56 (0.11)
−1	0.73 (0.11)	0.60 (0.10)	0.77 (0.14)	0.82 (0.12)	0.77 (0.09)	0.67 (0.25)

The average areas within absolute activation thresholds are given in mm^2 with SEM in parenthesis (n = 11 WT, 12 *reeler*).

response was somewhat smaller in *reeler* than in WT mice, but this effect was not statistically significant (2-way ANOVA with repeated measures, genotype and frequency; effect of frequency, $P < 0.001$; no effect of genotype, $P = 0.71$; no genotype × Frequency interaction, $P = 0.67$; $n = 11$ WT and 12 *reeler*). We conclude that under similar experimental conditions, the intrinsic signals evoked by single-whisker stimulation are comparable across the range of frequencies we tested. Therefore, in spite of the loss of lamination and resulting cortical disorganization, cortical processing of sensory information in the barrel cortex as measured with intrinsic imaging seems indistinguishable between *reeler* and WT.

Tactile information in the rodent whisker to barrel pathway reaches the somatosensory cortex primarily through thalamocortical synapses clustering in LIV barrels. From there, information spreads vertically through intracolumnar projections from LIV to the supra- and infragranular layers, but also horizontally through transcolumnar projection originating in LII/III, IV, and V (Petersen and Sakmann 2001; Schubert et al. 2007). The sensory evoked intrinsic signals we recorded in our experiments covered an area spanning several barrels (Fig. 3*A*,*C*), and most likely represent the horizontal span of effective corticocortical connections conveying information to neighboring columns. Differences in the size of the area activated by whisker stimulation may therefore provide evidence of altered transcolumnar connectivity in the disturbed cortex of the *reeler* mutant. In order to address this issue, we measured the area contained within fixed activation thresholds (1 to 5 × 10e−4) and compared both genotypes on that basis (Fig. 4*A*,*C* and Table 1). Statistical analysis (2-way ANOVA, genotype and threshold) was carried out separately for each frequency. We consistently found an effect of the threshold on the area ($P < 0.01$ for all frequencies, $n = 11$ WT and 12 *reeler*) but not of the genotype ($P = 0.12$; $P = 0.09$ and $P = 0.35$ for 5, 10, and 25 Hz, respectively) and no genotype × threshold interactions ($P = 0.99$; $P = 0.97$ and $P = 0.96$ for 5, 10, and 25 Hz, respectively). These results do not support the hypothesis that *reeler* transcolumnar connectivity differs from WT in its horizontal reach.

Cortical Vasculature in Reeler *and WT Mice*

As a functional imaging technique, optical imaging of intrinsic signals measures multicomponent hemodynamic signals including hemoglobin oxygenation level, blood flow, and volume (Malonek et al. 1997; Vanzetta and Grinvald 2008). Functional mapping with such a technique depends critically on there being a densely interconnected microvascular network in the cortical area under scrutiny, capable of supplying blood to regions of heightened neuronal activity with a high spatial fidelity. Can the loss of reelin and the ensuing disturbance in neocortical development also alter the development and patterning of the cortical vascular bed? We sought to answer this question by staining coronal sections of WT and *reeler* animals with DAB, which reveals the hydrogen peroxidase rich erythrocytes left in the cortical vessels after immersion fixation and provides a suitable surrogate staining for blood vessels in sections of adult mouse cortex (Fig. 5*A*,*B*). We measured the density of blood vessels contained in the cortex in 100 μm bins, starting 100 μm below the pia because of the higher background staining immediately below the pia. Results are shown in Figure 5*C*. The distribution of blood vessels in WT broadly varied with increasing depth, with the supragranular layers containing a higher density of vessels than the infragranular layers. Vascular density peaked at a depth of 300–400 μm, which extended across the LII/III to LIV border into LIV in our sections. The vascular density was significantly higher at depth of 200–400 μm than at depths of 700–1000 μm (ANOVA, $P < 0.05$ in all tests). The vascular density in *reeler* mice followed a similar distribution along the depth of the cortex, peaked at a depth of 300–400 μm, but there was no significant difference in the density of blood vessel at different depths. Hence, the distribution of blood vessels across the cortical depth in *reeler* cortex varies within a narrower spectrum but follows the same pattern than in WT. Thus, the results obtained with intrinsic imaging are unlikely to be skewed by differences in brain perfusion related to distinct anatomical organizations of the cortical vasculature in *reeler* and WT.

Discussion

The Reeler *Barrel Cortex Maintains a Somatotopic Representation of the Sensory Periphery*

We used in vivo ISOI to compare the disorganized, nonlaminated barrel cortex of *reeler* animals to its highly organized counterpart in WT in terms of sensory map organization and activation. To the best of our knowledge, we hereby provide the first demonstration of somatotopy in the *reeler* barrel cortex from in vivo functional imaging. This result reflects the existence of an orderly columnar organization in the absence of cortical layers in *reeler* (Dekimoto et al. 2010; Wagener et al. 2010; Boyle et al. 2011), as the barrel field remains visible in tangential sections through the *reeler* somatosensory cortex. The persistence of a correct, functional somatotopic sensory map implies that thalamocortical fibers originating from barreloids within the ventrobasal thalamic nucleus manage to find their appropriate target columns in *reeler* animals.

As demonstrated in the present study, stimulation of an individual vibrissa evokes a hemodynamic signal centered on, and

peaking at, the location of the corresponding barrel in the barrel field, indicating that neurons sharing similar receptive field properties are also grouped into barrel-related columns in the somatosensory cortex of the *reeler* mouse and demonstrating that information flow into the cortex retains a columnar organizing principle in the otherwise disorganized *reeler* cortex (Mountcastle et al. 1955; Mountcastle 1957, 1997; Petersen and Sakmann 2001; Horton and Adams 2005; Feldmeyer et al. 2013). During cortical development, newly generated neurons deriving from common progenitors migrate radially into the cortex where they form networks of sibling neurons sharing similar receptive field properties, and the *reeler* functional columnar modules revealed by the present study are therefore likely to be composed of neurons sharing a common lineage (Rakic 1988; Yu et al. 2012; Li et al. 2012). Together with the correct positioning of the somatosensory cortex within the cortical mantle, this observation can be reconciled with the view that cortical development involves the projection of an arealized protomap already existing at the level of the early proliferative cortical sheet onto the developing cortical plate through the radial migration of newborn neurons, since only the radial, and not tangential, organization of the barrel field is compromised in *reeler* (Rakic 1988). According to this view, while cortical arealization is determined by the arealization of the proliferative cortical sheet itself, the size or number of columns assigned to a given cortical area can be further modulated by thalamic input (Rakic 1988; Sur and Rubenstein 2005). Interestingly, the PMBSF in *reeler* occupies a proportionally larger area of the cortical mantle than in WT, mainly due to an increase in the size of the septal compartment (Wagener et al. 2010). In addition, although thalamocortical axons seem to find their appropriate targets in *reeler*, some abnormalities in their trajectories within the cortex have been documented, such as the oblique rather than straight angle at which they arise from the white matter towards the pia and their subsequent descent towards their terminal fields (Caviness and Frost 1983; Harsan et al. 2013).

Stimulus Representation and Cortical Connectivity in Barrel Cortex

How comparable is the cortical connectivity underlying the intrinsic signals that we observed in *reeler* and WT animals? Previous studies have reported abnormal connectivity in the *reeler* brain outside of the somatosensory cortex. Ectopic and heterologous synapses have been described in the cerebellum, such as synapses formed by mossy fibers on Purkinje cells in *reeler* cerebellum with no equivalent in WT (Mariani et al. 1977; Wilson et al. 1981; Sotelo 1990). In the hippocampus of *reeler*, a fraction of fibers from the entorhino-hippocampal pathway are found in ectopic position and innervate inappropriate layers (Borrell et al. 1999). These ectopic fibers are likely to form functional synapses, and a fraction of mossy cells have indeed been found to receive aberrant, direct input from fibers of the perforant path (Kowalski et al. 2010). Furthermore, in the same study, mossy cells which do not receive direct input from the perforant path have been found to respond with a much lower temporal precision to disynaptic activation through stimulation of the perforant path than their WT equivalents. These results indicate that as a population, mossy cells are likely to fire in a much more asynchronous manner in *reeler* with respect to WT, leading to the notion that proper hippocampal network function might be compromised in *reeler*.

Should similar abnormalities occur in *reeler* somatosensory cortex, they would raise the question of whether network function remains similar to WT, and first and foremost, whether similar sensory input would be able to drive cortical network activity in an appropriate manner. Although no formal proof of aberrant connectivity in *reeler* somatosensory cortex is available as of yet, the existence of aberrant connections has been postulated (Caviness and Rakic 1978; Caviness and Frost 1983). Interestingly, in the *reeler* visual cortex, a comparatively larger fraction of neurons are responding only poorly to visual stimulation, as could conceivably occur if either the thalamocortical input or its amplification within the cortex were weaker (Dräger 1981; Lien and Scanziani 2013).

In the present study, we used ISOI to measure the cortical response to a controlled sensory stimulation. The sensory evoked hemodynamic signals did not differ in amplitude between both genotypes, which is likely to reflect the fact that thalamocortical input to both cortices was similar under our experimental conditions. In addition, we found that single vibrissa stimulation evokes a hemodynamic response that spreads further horizontally than the size of the corresponding barrel to encompass a large fraction of the barrel field, in agreement with previous reports (Masino et al. 1993; Chen-Bee et al. 1996, 2012; Drew and Feldman. 2009). Our intrinsic signals were acquired from a depth of 300 μm below the pia, implying that our signals were dominated by granular and supragranular layer sources in WT animals. Tactile information reaches the somatosensory cortex through thalamocortical synapses clustering in LIV barrels. From there, excitation spreads vertically to and horizontally within LII/III to neighboring columns, presumably through transcolumnar excitatory connections originating from LIV and LII/III. A similar phenomenon occurs in LV, resulting in an hourglass-shaped profile of neuronal excitation spread, encompassing a barrel and a large domain of supra-and infragranular layers (Kohn et al. 2000; Petersen and Sakmann 2001, 2007; Schubert et al. 2007). This horizontal spread of excitation causes single-whisker stimulation to evoke hemodynamic signals that cover more than the size of their corresponding barrel to actually encompass a large fraction of the barrel field, similar to what can be observed with voltage-sensitive dye imaging (Ferezou et al. 2006). In *reeler* mice, LII/III and LV fated cells are spread across the depth of the cortex instead of forming distinct layers (Wagener et al. 2010). Because we found no increase (or decrease) in the area covered by the sensory evoked intrinsic signal in *reeler* animals, we suggest that transcolumnar corticocortical connections innervate a domain that is similar in size to what is observed in a laminated cortex.

In summary, we found no significant differences in the spatiotemporal spread or amplitude of cortical representation of controlled sensory inputs as measured by ISOI. We postulate that the responsiveness of cortical networks to thalamocortical input is unchanged in the *reeler* somatosensory cortex, and we would argue that abnormalities in corticocortical connectivity within the barrel field or electrophysiological properties of individual neurons are likely to be marginal. Although experimental evidence for this claim is still lacking, several studies have shown that long-distance connectivity indeed remains intact in *reeler* animals (Steindler and Colwell 1976; Yamamoto et al. 2003).

Neurovascular Response Function in Reeler

A drawback of functional imaging techniques applied to the study of cortical networks is that the neurovascular response function, or quantitative relationship between any given amount of evoked neuronal activity and the corresponding hemodynamic signals being recorded, is not known explicitly in every experimental condition. Yet without this knowledge, the interpretation of hemodynamic signals with respect to the underlying neuronal processes they represent is delicate. The most straightforward way to estimate the response function is to obtain both a measure of neuronal activity and a hemodynamic signal in similar experimental conditions (if not outright simultaneously). Experiments of this type have demonstrated that the neurovascular response function can be affected by anesthesia (Martin et al. 2006) and differs depending on the anatomical structure under investigation (Devonshire et al. 2012). Can the response function be affected by the loss of function of reelin and the subsequent loss of cortical lamination as well? While the current study does not include a direct measure of evoked neuronal activity, further evidence that the cortex responds to sensory stimulation in *reeler* animals exists in the literature. Using a detailed analysis of c-fos staining as a measure of neuronal activity in mice upon exploration of an enriched environment, our group found no difference between *reeler* and WT animals in c-fos expression levels, suggesting that the neuronal networks in these genotypes do not differ in terms of large-scale activation in response to a whisker-dependent behavior (Wagener et al. 2010). Furthermore, extracellular recordings in the visual cortex demonstrated that transcallosal and corticotectal neurons in the primary visual area have comparable receptive field properties in both genotypes (Lemmon and Pearlman 1981; Simmons and Pearlman 1983). These lines of evidence suggest that behavioral activation of sensory cortex obeys comparable rules in *reeler* and WT mice. Following this assumption, the most parsimonious explanation for the lack of difference in the amplitude of the sensory evoked hemodynamic signals reported in this study is that the hemodynamic response function is largely unaffected by the loss of either reelin or cortical lamination. We therefore propose that the same tactile stimulation evokes comparable neuronal activity and hemodynamic signals in both genotypes under our experimental conditions.

The results from our imaging experiments did not seem to be skewed by large differences in the layout of the microvascular network underlying the intrinsic signal between genotypes. Using a staining protocol which labels erythrocytes rather than blood vessels, we were able to indirectly reveal the microvascular architecture in the somatosensory cortex, and found that the relative density of blood vessels peaks at a depth of ~300–400 μm below the pia, roughly corresponding to lower LII/III and upper LIV in our sections. These results are in agreement with those obtained with high-throughput, automated histology coupled with extensive labeling of the cortical microvascular network (Blinder et al. 2013). In line with a previous qualitative investigation, we found no large quantitative difference in the architecture of the microvascular network in *reeler* compared with WT animals (Stubbs et al. 2009). It appears, therefore, that the loss of either reelin or cortical layers does not strongly affect the development of a dense cortical blood vessel network.

In summary, we investigated the sensory map organization and function of the *reeler* somatosensory cortex in vivo and found little difference with a WT cortex. Previous studies have established that only minor abnormalities exist in electrophysiological properties of single neurons in the *reeler* cortex (Dräger 1981; Lemmon and Pearlman 1981; Simmons and Pearlman 1983). To our knowledge, behavioral investigations of the *reeler* mutant have not revealed obvious somatosensory deficits (Salinger et al. 2003). Taken together, these results indicate that *reeler* brain retains a proper function of sensory systems and therefore raise the intriguing possibility that while columnar organization of cortical networks is a ubiquitous feature of the cortex relevant to our understanding of its function, the subsequent subdivision of columnar networks into layer-specific compartments may not represent an absolute necessity for proper cortical function (Schubert et al. 2007). In such a view, lamination of the cortex could be seen as an incidental consequence of the sequential nature of neuronal birth and migration, perhaps corresponding to a developmental strategy aimed at optimizing wiring costs, rather than a prerequisite for the establishment of computationally effective cortical networks (Chklovskii 2004; Wen and Chklovskii 2008). More detailed experimental approaches are necessary however, before we can fully elucidate the impact of the loss of lamination on information flow in the barrel cortex and its putative behavioral consequences, based for instance on functional imaging and single cell electrophysiology on acute thalamocortical slices (Petersen and Sakmann 2001; Petreanu et al. 2009; Kowalski et al. 2010) as well as whisker related behavioral paradigms in head restrained animals (O'Connor et al. 2010). Finally, the present results lend support to the notion that appropriate thalamocortical and corticocortical connections are established in *reeler* animals in spite of the loss of cortical lamination characteristic of this mutant (Harsan et al. 2013). It thus appears that a surprisingly extensive structural and functional plasticity enables the *reeler* brain to retain a basic functionality of sensory systems, although not of higher cognitive processing (Salinger et al. 2003), an interesting mismatch that remains to be understood.

Funding

This work was supported by the Deutsche Forschungsgemeinschaft (DFG) via the CRC 889 (Project C3). Funding to pay the Open Access publication charges for this article was provided by the DFG via the CRC 889.

Notes

We are grateful to Dr Ivo Vanzetta for skillful introduction to intrinsic signal optical imaging, to Prof. Siegrid Löwel and Prof. Tim Gollisch for constructive counseling on the design of the analysis, and to Patricia Sprysch for excellent technical assistance. We address our thanks to the Institut für Medizinische Statistik of the Georg-August Universität for their advice on statistics. *Conflict of Interest:* None declared.

References

Armstrong-James M, Fox K. 1987. Spatiotemporal convergence and divergence in the rat S1 "barrel" cortex. J Comp Neurol. 263 (2):265–281.

Blinder P, Tsai PS, Kaufhold JP, Knutsen PM, Suhl H, Kleinfeld D. 2013. The cortical angiome: an interconnected vascular network with noncolumnar patterns of blood flow. Nat Neurosci. 16 (7):889–897.

Borrell V, Del Río JA, Alcántara S, Derer M, Martínez A, D'Arcangelo G, Nakajima K, Mikoshiba K, Derer P, Curran T et al. 1999. Reelin

regulates the development and synaptogenesis of the layer-specific entorhino-hippocampal connections. J Neurosci. 19(4):1345–1358.
Boyle MP, Bernard A, Thompson CL, Ng L, Boe A, Mortrud M, Hawrylycz MJ, Jones AR, Hevner RF, Lein ES. 2011. Cell-type-specific consequences of Reelin deficiency in the mouse neocortex, hippocampus, and amygdala. J Comp Neurol. 519(11):2061–2089.
Brecht M, Preilowski B, Merzenich MM. 1997. Functional architecture of the mystacial vibrissae. Behav Brain Res. 84(1–2):81–97.
Carvell GE, Simons DJ. 1990. Biometric analyses of vibrissal tactile discrimination in the rat. J Neurosci. 10(8):2638–2648.
Caviness VS Jr, Frost DO, Hayes NL. 1976. Barrels in somatosensory cortex of normal and reeler mutant mice. Neurosci Lett. 3(1–2):7–14.
Caviness VS Jr, Frost DO. 1983. Thalamocortical projections in the reeler mutant mouse. J Comp Neurol. 219(2):182–202.
Caviness VS Jr, Rakic P. 1978. Mechanisms of cortical development: a view from mutations in mice. Annu Rev Neurosci. 1:297–326. Review.
Chen-Bee CH, Kwon MC, Masino SA, Frostig RD. 1996. Areal extent quantification of functional representations using intrinsic signal optical imaging. J Neurosci Methods. 68(1):27–37.
Chen-Bee CH, Polley DB, Brett-Green B, Prakash N, Kwon MC, Frostig RD. 2000. Visualizing and quantifying evoked cortical activity assessed with intrinsic signal imaging. J Neurosci Methods. 97 (2):157–173.
Chen-Bee CH, Zhou Y, Jacobs NS, Lim B, Frostig RD. 2012. Whisker array functional representation in rat barrel cortex: transcendence of one-to-one topography and its underlying mechanism. Front Neural Circuits. 6:93.
Chklovskii DB. 2004. Synaptic connectivity and neuronal morphology: two sides of the same coin. Neuron. 43(5):609–617.
Dekimoto H, Terashima T, Katsuyama Y. 2010. Dispersion of the neurons expressing layer specific markers in the reeler brain. Dev Growth Differ. 52(2):181–193.
Devonshire IM, Papadakis NG, Port M, Berwick J, Kennerley AJ, Mayhew JE, Overton PG. 2012. Neurovascular coupling is brain region-dependent. NeuroImage. 59(3):1997–2006.
Diamond ME, Arabzadeh E. 2013. Whisker sensory system—from receptor to decision. Prog Neurobiol. 103:28–40.
Diamond ME, von Heimendahl M, Knutsen PM, Kleinfeld D, Ahissar E. 2008. "Where" and "what" in the whisker sensorimotor system. Nat Rev Neurosci. 9(8):601–612.
Dräger UC. 1981. Observations on the organization of the visual cortex in the reeler mouse. J Comp Neurol. 201(4):555–570.
Drew PJ, Feldman DE. 2009. Intrinsic signal imaging of deprivation-induced contraction of whisker representations in rat somatosensory cortex. Cereb Cortex. 19(2):331–348.
Dubroff JG, Stevens RT, Hitt J, Hodge CJ Jr, McCasland JS. 2006. Anomalous functional organization of barrel cortex in GAP-43 deficient mice. Neuroimage. 29(4):1040–1048.
D'Arcangelo G, Miao GG, Chen SC, Soares HD, Morgan JI, Curran T. 1995. A protein related to extracellular matrix proteins deleted in the mouse mutant reeler. Nature. 374(6524):719–723.
Falconer DS. 1951. Two new mutants, "trembler" and "reeler", with neurological actions in the house mouse (*Mus musculus* L.). J Genet. 50:192–201.
Feldmeyer D, Brecht M, Helmchen F, Petersen CC, Poulet JF, Staiger JF, Luhmann HJ, Schwarz C. 2013. Barrel cortex function. Prog Neurobiol. 103:3–27.
Ferezou I, Bolea S, Petersen CC. 2006. Visualizing the cortical representation of whisker touch: voltage-sensitive dye imaging in freely moving mice. Neuron. 50(4):617–629.
Frostig RD, Lieke EE, Ts'o DY, Grinvald A. 1990. Cortical functional architecture and local coupling between neuronal activity and the microcirculation revealed by in vivo high-resolution optical imaging of intrinsic signals. Proc Natl Acad Sci U S A. 87(16):6082–6086.
Goffinet AM. 1984. Events governing organization of postmigratory neurons: studies on brain development in normal and reeler mice. Brain Res. 319:261–296.
Grinvald A, Lieke E, Frostig RD, Gilbert CD, Wiesel TN. 1986. Functional architecture of cortex revealed by optical imaging of intrinsic signals. Nature. 324(6095):361–364.
Harsan LA, Dávid C, Reisert M, Schnell S, Hennig J, von Elverfeldt D, Staiger JF. 2013. Mapping remodeling of thalamocortical projections in the living reeler mouse brain by diffusion tractography. Proc Natl Acad Sci U S A. 110(19):E1797–E1806.
Horton JC, Adams DL. 2005. The cortical column: a structure without a function. Philos Trans R Soc Lond B Biol Sci. 360(1456):837–862. Review.
Kohn A, Metz C, Quibrera M, Tommerdahl MA, Whitsel BL. 2000. Functional neocortical microcircuitry demonstrated with intrinsic signal optical imaging in vitro. Neuroscience. 95(1):51–62.
Kowalski J, Geuting M, Paul S, Dieni S, Laurens J, Zhao S, Drakew A, Haas CA, Frotscher M, Vida I. 2010. Proper layering is important for precisely timed activation of hippocampal mossy cells. Cereb Cortex. 20(9):2043–2054.
Lemmon V, Pearlman AL. 1981. Does laminar position determine the receptive field properties of cortical neurons? A study of corticotectal cells in area 17 of the normal mouse and the reeler mutant. J Neurosci. 1(1):83–93.
Li Y, Lu H, Cheng PL, Ge S, Xu H, Shi SH, Dan Y. 2012. Clonally related visual cortical neurons show similar stimulus feature selectivity. Nature. 486(7401):118–121.
Lien AD, Scanziani M. 2013. Tuned thalamic excitation is amplified by visual cortical circuits. Nat Neurosci. 16(9):1315–1323.
Madisen L, Zwingman TA, Sunkin SM, Oh SW, Zariwala HA, Gu H, Ng LL, Palmiter RD, Hawrylycz MJ, Jones AR et al. 2010. A robust and high-throughput Cre reporting and characterization system for the whole mouse brain. Nat Neurosci. 13(1):133–140.
Malonek D, Dirnagl U, Lindauer U, Yamada K, Kanno I, Grinvald A. 1997. Vascular imprints of neuronal activity: relationships between the dynamics of cortical blood flow, oxygenation, and volume changes following sensory stimulation. Proc Natl Acad Sci U S A. 94 (26):14826–14831.
Mariani J, Crepel F, Mikoshiba K, Changeux JP, Sotelo C. 1977. Anatomical, physiological and biochemical studies of the cerebellum from Reeler mutant mouse. Philos Trans R Soc Lond B Biol Sci. 281 (978):1–28.
Martin C, Martindale J, Berwick J, Mayhew J. 2006. Investigating neural-hemodynamic coupling and the hemodynamic response function in the awake rat. NeuroImage. 32(1):33–48.
Masino SA, Kwon MC, Dory Y, Frostig RD. 1993. Characterization of functional organization within rat barrel cortex using intrinsic signal optical imaging through a thinned skull. Proc Natl Acad Sci U S A. 90(21):9998–10002.
Mayhew JE, Askew S, Zheng Y, Porrill J, Westby GW, Redgrave P, Rector DM, Harper RM. 1996. Cerebral vasomotion: a 0.1-Hz oscillation in reflected light imaging of neural activity. NeuroImage. 4(3 Pt 1):183–193.
Mountcastle VB. 1957. Modality and topographic properties of single neurons of cat's somatic sensory cortex. J Neurophysiol. 20 (4):408–434.
Mountcastle VB. 1997. The columnar organization of the neocortex. Brain. 120(Pt 4):701–722. Review.
Mountcastle VB, Berman AL, Davies PW. 1955. Topographic organization and modality representation in first somatic area of cat's cerebral cortex by method of single unit analysis. Am J Physiol. 183:464.
O'Connor DH, Clack NG, Huber D, Komiyama T, Myers EW, Svoboda K. 2010. Vibrissa-based object localization in head-fixed mice. J Neurosci. 30(5):1947–1967.
Petersen CC. 2007. The functional organization of the barrel cortex. Neuron. 56(2):339–355.
Petersen CC, Sakmann B. 2001. Functionally independent columns of rat somatosensory barrel cortex revealed with voltage-sensitive dye imaging. J Neurosci. 21(21):8435–8446.
Petreanu L, Mao T, Sternson SM, Svoboda K. 2009. The subcellular organization of neocortical excitatory connections. Nature. 457 (7233):1142–1145.
Polleux F, Dehay C, Kennedy H. 1998. Neurogenesis and commitment of corticospinal neurons in reeler. J Neurosci. 18:9910–9923.
Polley DB, Kvasnák E, Frostig RD. 2004. Naturalistic experience transforms sensory maps in the adult cortex of caged animals. Nature. 429(6987):67–71.

Rakic P. 1988. Specification of cerebral cortical areas. Science. 241 (4862):170–176. Review.
Rubin BD, Katz LC. 1999. Optical imaging of odorant representations in the mammalian olfactory bulb. Neuron. 23(3):499–511.
Salinger WL, Ladrow P, Wheeler C. 2003. Behavioral phenotype of the reeler mutant mouse: effects of RELN gene dosage and social isolation. Behav Neurosci. 117(6):1257–1275.
Schubert D, Kötter R, Staiger JF. 2007. Mapping functional connectivity in barrel-related columns reveals layer- and cell type-specific microcircuits. Brain Struct Funct. 212(2):107–119.
Schuett S, Bonhoeffer T, Hübener M. 2002. Mapping retinotopic structure in mouse visual cortex with optical imaging. J Neurosci. 22 (15):6549–6559.
Simmons PA, Pearlman AL. 1983. Receptive-field properties of transcallosal visual cortical neurons in the normal and reeler mouse. J Neurophysiol. 50(4):838–848.
Sotelo C. 1990. Cerebellar synaptogenesis: what we can learn from mutant mice. J Exp Biol. 153:225–249. Review.
Steindler DA, Colwell SA. 1976. Reeler mutant mouse: maintenance of appropriate and reciprocal connections in the cerebral cortex and thalamus. Brain Res. 113(2):386–393.
Stubbs D, DeProto J, Nie K, Englund C, Mahmud I, Hevner R, Molnár Z. 2009. Neurovascular congruence during cerebral cortical development. Cereb Cortex. 19(Suppl 1):i32–i41.
Sur M, Rubenstein JL. 2005. Patterning and plasticity of the cerebral cortex. Science. 310(5746):805–810. Review.
Tissir F, Goffinet AM. 2003. Reelin and brain development. Nat Rev Neurosci. 4(6):496–505.
Vanzetta I, Grinvald A. 2008. Coupling between neuronal activity and microcirculation: implications for functional brain imaging. HFSP J. 2(2):79–98.
Wagener RJ, Dávid C, Zhao S, Haas CA, Staiger JF. 2010. The somatosensory cortex of reeler mutant mice shows absent layering but intact formation and behavioural activation of columnar somatotopic maps. J Neurosci. 30(46):15700–9.
Welker C. 1976. Receptive fields of barrels in the somatosensory neocortex of the rat. J Comp Neurol. 166(2):173–189.
Welker C, Woolsey TA. 1974. Structure of layer IV in the somatosensory neocortex of the rat: description and comparison with the mouse. J Comp Neurol. 158(4):437–453.
Wen Q, Chklovskii DB. 2008. A cost-benefit analysis of neuronal morphology. J Neurophysiol. 99(5):2320–2328.
White BR, Bauer AQ, Snyder AZ, Schlaggar BL, Lee JM, Culver JP. 2011. Imaging of functional connectivity in the mouse brain. PLoS One. 6(1):e16322.
Wilson L, Sotelo C, Caviness VS Jr. 1981. Heterologous synapses upon Purkinje cells in the cerebellum of the Reeler mutant mouse: an experimental light and electron microscopic study. Brain Res. 213(1):63–82.
Wong-Riley MT, Welt C. 1980. Histochemical changes in cytochrome oxidase of cortical barrels after vibrissal removal in neonatal and adult mice. Proc Natl Acad Sci U S A. 77(4):2333–2337.
Woolsey TA, Van der Loos H. 1970. The structural organization of layer IV in the somatosensory region (SI) of mouse cerebral cortex. The description of a cortical field composed of discrete cytoarchitectonic units. Brain Res. 17(2):205–242.
Yamamoto T, Sakakibara S, Mikoshiba K, Terashima T. 2003. Ectopic corticospinal tract and corticothalamic tract neurons in the cerebral cortex of yotari and reeler mice. J Comp Neurol. 461(1):61–75.
Yu YC, He S, Chen S, Fu Y, Brown KN, Yao XH, Ma J, Gao KP, Sosinsky GE, Huang K et al. 2012. Preferential electrical coupling regulates neocortical lineage-dependent microcircuit assembly. Nature. 486 (7401):113–117.